



ELSEVIER

Available online at www.sciencedirect.com

SCIENCE @ DIRECT®

Journal of Organometallic Chemistry 681 (2003) 158–166

Journal
of Organo
metallic
Chemistrywww.elsevier.com/locate/jorganchem

Study of the self-assembly reactions between the organic linker 1,4-bis(4-pyridyl)butadiyne and the metal-containing corners (diphosphine)M(II) (M = Pd, Pt; diphosphine = dppp, dppf, depe, dppbz)

Montserrat Ferrer*, Laura Rodríguez, Oriol Rossell

Departament de Química Inorgànica, Universitat de Barcelona, Martí i Franquès 1, Barcelona 08028, Spain

Received 30 May 2003; received in revised form 20 June 2003; accepted 20 June 2003

Abstract

The diaza ligand 1,4-bis(4-pyridyl)butadiyne (**L**) has been used as a linker in self-assembly reactions with different diphosphine Pd(II) and Pt(II) triflates to build metallosupramolecular squares and triangles. Equilibria between triangular and square entities have been detected in most of the cases and their composition studied by multinuclear NMR spectroscopy and mass spectrometry. The self-assembly process has been shown to be strongly dependent on the conditions of the medium and the nature of the transition metal. The ability of some of these compounds to recognise inorganic anions has been investigated.

© 2003 Elsevier B.V. All rights reserved.

Keywords: Supramolecular chemistry; Self-assembly; Molecular recognition; Platinum; Palladium; Diphosphine

1. Introduction

Since Fujita et al. [1] reported the first example of a self-assembled square metallosupramolecule, there have appeared many molecular squares where 90° angles at the four edges of the polygon are provided by transition metals, hypervalent iodine or organic frameworks [2]. Although self-assembled molecular squares are expected from the combination of right-angular components and linear ditopic units, the simultaneous self-assembly of molecular triangles has recently been observed [3]. Both products are in equilibrium with each other, which is concentration-dependent: at higher concentration, the ratio shifts toward the molecular square, according to Le Chatelier's law. As a consequence of this behaviour, these systems have been a topic in recent years due to their potential insight into the mechanism of self-assembly. It has been pointed out that the driving force for the self-assembly process is under thermodynamic

control [4]: molecular squares are less strained and hence more stable in terms of enthalpy, while entropic factors favour the triangle since it is assembled from fewer components. In this context, the equilibrium observed in a number of examples evidences that both products should be close together in energy. Thus, subtle changes in the nature of the molecular components (organic linear linkers or metal corner units) determine which species are formed and where the equilibrium lies. Selected examples concerning only palladium or platinum derivatives will help to show the complexity of this kind of processes: (i) a molecular square was obtained by self-assembly from [Pd(NO₃)₂(en)] and 4,4'-bipyridine, while the use of the longer ligands py-X-py (py = 4-pyridyl; X = CH=CH, C≡C, *p*-C₆H₄) gave a mixture of square and triangular species [3a]; (ii) if the ethylenediamine group on palladium is replaced with the more sterically demanding 2,2'-bipyridine, the resulting square with 4,4'-bipyridine was also in equilibrium with the corresponding molecular triangle [3a]; (iii) an unexpected supramolecular triangle composed of the ditopic donor pyrazine and *cis*-Pt(PMe₃)₂ was obtained as a unique species [5]; (iv) *cis*-Pt(dppp) and linear

* Corresponding author. Tel.: +34-93-402-12-74; fax: +34-93-490-77-25.

E-mail address: montse.ferrer@qi.ub.es (M. Ferrer).

diazaligands were reported to form either exclusively molecular squares [2] or square–triangle equilibria [3d,3e,6] depending on the nature of the bridging ligand; (v) the reaction of the *cis*-Pt(dppf) corner with 2,7-diazapyrene permitted the synthesis of a “pure” square molecular species [7] while its reaction with the organic edge 1,4-bis(4-pyridyl)tetrafluorobenzene gave a mixture of square and triangular supramolecules in equilibrium [6]. This unexpected set of results makes it currently difficult to predict the nature of the resulting self-assembled products, and although extended and constitutionally flexible organic edges have been postulated to favour the self-assembly of triangular supramolecules [2b], a number of processes do not fulfil this condition [5,8]. In order to gain insight into this chemistry, we report here the reaction of *cis*-M(II)(diphosphine) (M = Pd or Pt; diphosphine = dppp (1,3-bis(diphenylphosphino)propane), dppf (1,1'-bis(diphenylphosphino)ferrocene), depe (1,2-bis(diethylphosphino)ethane) and dppbz (1,2-bis(diphenylphosphino)benzene) with the diazaligand 1,4-bis(4-pyridyl)butadiyne (**L**). In most of the cases, concentration-dependent triangle–square equilibria were observed and their composition studied.

2. Results and discussion

We aimed at the construction of a series of self-assembled supramolecular species of palladium and platinum via *cis*-M(II)(diphosphine) and the diazaligand **L** whose ability to give molecular polygons had been reported earlier [3a,9]. Before discussing the experimental results, we should point out that we initially assumed that the geometry of the self-assembled molecular polygons depended, in part, on the nature of the diphosphine ligands. Experimental and theoretical results reported by us [6] have demonstrated that *cis*-M(dppf) corners showed a marked preference for the formation of triangular supramolecules in their reactions with the fluorinated ligand, 1,4-bis(4-pyridyl)tetrafluorobenzene, while *cis*-M(dppp) corners yielded predominantly square species instead. Moreover, in the case of *cis*-M(depe), the ratio square/triangle has been observed to be extremely concentration-dependent in accordance with the calculated small energy difference between the two polygons. Because of all this, we designed a series of experiments including different metal corners, i.e. *cis*-M(diphosphine) (diphosphine = dppp, dppf, depe and dppbz), and the same ditopic ligand **L**. Although both **L** and our fluorinated ligand are stereochemically rigid, they present different lengths and electronic characteristics. This fact could have an influence on the nature of the self-assembled species.

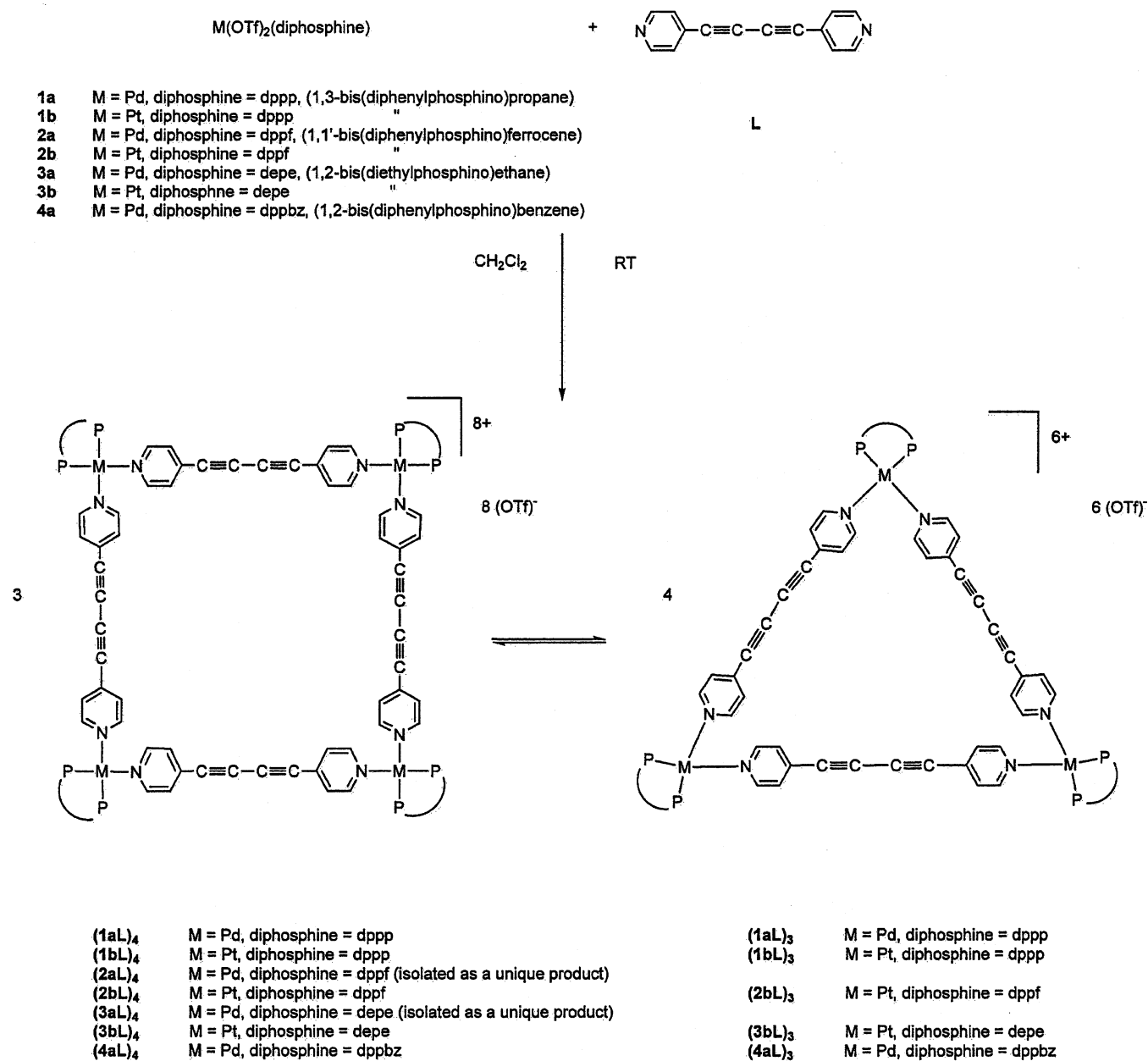
2.1. Preparation and characterisation of metallacycles

The corner units *cis*-M(II)(diphosphine) were synthesised by reaction of the transition metal halides [MX₂(diphosphine)] with an excess of silver triflate in the appropriate organic solvent. Palladium and platinum corners containing dppf, dppp and depe have been successfully used for the synthesis of molecular polygons by several authors while the more rigid *cis*-Pd(dppbz) has been employed in the work described here for the first time.

The construction of the new molecular species (Scheme 1) via self-assembly of **1–4a** and **1–3b** and **L** was achieved by mixing solutions of the metal complex and **L** at room temperature at three different concentrations (1, 10 and 100 mM) [10]. The reactions were monitored by ³¹P{¹H}-NMR spectroscopy and the results are given below.

The stoichiometric reaction of **1a** with **L** in CH₂Cl₂ at low concentration (1 mM) gave, within the detection limits, only a single product ($\delta(^{31}\text{P}) = 8.0$ ppm) which was assigned to the triangular species. ¹H-NMR spectroscopy also showed only one set of signals corresponding to the α - and β -protons of the aromatic ligand **L** that appeared well resolved. This assignment is strongly supported by concentration effects. Thus, repeating the experience at 10 mM concentration, two products were evidenced by ³¹P{¹H}-NMR spectroscopy, one corresponding to the triangular species ($\delta(^{31}\text{P}) = 8.0$ ppm) and the other due to a symmetrical compound ($\delta(^{31}\text{P}) = 7.4$ ppm) that was assigned to the square molecular species. The reaction was carried out at even higher concentration (100 mM) and in this case a single peak in the ³¹P{¹H}-NMR spectrum at $\delta = 7.4$ ppm was observed (square). This fact confirmed the correct assignment of the species. This is notable because of the way the adopted geometry is clearly influenced by the concentration of the solution, that is, the triangular form appears at low concentrations while the square entity is not only the predominant but the only species in solution at high concentration. The integral ratio of the ³¹P{¹H}-NMR signals was found to be temperature-dependent changing from approximately 1:1 (triangular/square molar ratio) at 273 K to about 2:1 at 313 K (10 mM solution), this process being reversible and in good accord with the Le Chatelier's law (Fig. 1).

The NMR spectra of the platinum species, resulting from reaction of **1b** with **L**, exhibited the same features as those of palladium ones, that is, concentration dependence, but in this case we were not able to obtain “pure” species in solution. Although the predominant product at low concentration (1 mM) was the triangle (**1bL**)₃ ($\delta(^{31}\text{P}) = -14.5$ ppm) and the square (**1bL**)₄ ($\delta(^{31}\text{P}) = -14.9$ ppm) at higher concentration (100 mM), in no case did the predominant species appear free from the other component. The same observations



Scheme 1.

were made by studying the equilibrium by either ^1H - or $^{195}\text{Pt}\{^1\text{H}\}$ -NMR spectroscopy. The peak at $\delta(^{195}\text{Pt}) = -4436$ ppm assigned to the triangular molecule shifted to $\delta(^{195}\text{Pt}) = -4421$ ppm (square unit) when the concentration of the solution was increased. It is remarkable that the ^{31}P resonances of the triangular species **(1aL)₃** and **(1bL)₃** appear downfield compared to that of **(1aL)₄** and **(1bL)₄**, respectively. The opposite trend was observed for the α -protons of the pyridine rings whose chemical shifts decreased in frequency going from the square to the triangular entity. A theoretical explanation of these trends (based on a GIAO-DFT study) has recently been given [6].

Notably, the equilibrium for the platinum complexes, **(1bL)₃** and **(1bL)₄**, is not perceptively temperature-dependent. Additional confirmation of the assignment of the compounds have been obtained from ES(+) mass spectrometry (see Section 3). Several attempts were made to obtain X-ray quality crystals, but while vapour diffusion of diethylether into nitromethane solutions produced crystals of **(1aL)₃**/**(1aL)₄** and **(1bL)₃**/**(1bL)₄** mixtures these proved to be highly unstable under diffraction conditions even at low temperatures.

Metal corners with the more flexible dppf ligand were also employed as component for self-assembly reactions with **L** and studied by NMR spectroscopy. The reaction

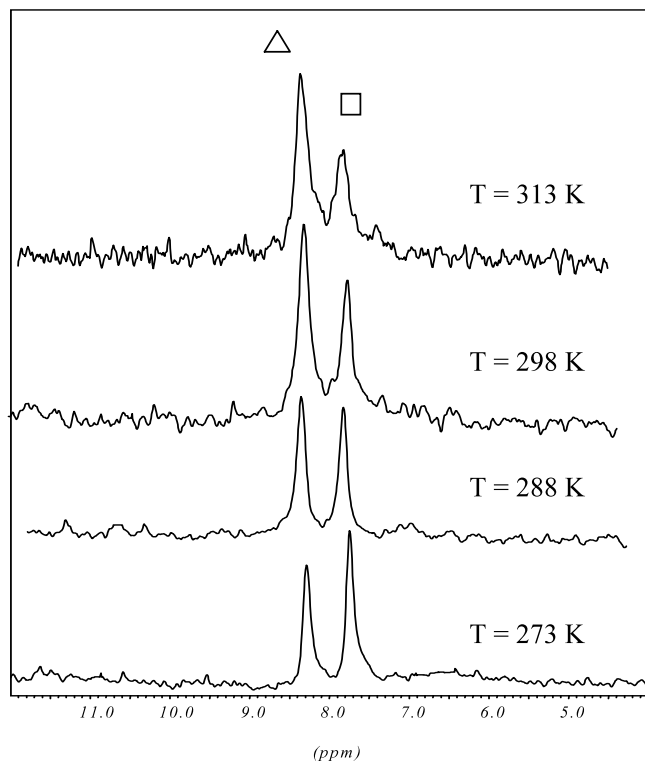


Fig. 1. $^{31}\text{P}\{^1\text{H}\}$ -NMR spectra of $(1\text{aL})_3/(1\text{aL})_4$ at different temperatures.

of the palladium complex **2a** with **L** gave rise to one species regardless of the concentration of the solution. We assigned that species to the square molecular compound $(2\text{aL})_4$ from the fragments detected in its ES(+) mass spectrum (e.g. $[\text{M}-5\text{OTf}]^{5+}$, $[\text{M}-3\text{OTf}]^{3+}$) (see Section 3). Moreover, controlled potential coulometry at 0.85 V using a platinum gauze electrode at room temperature indicated that four electrons are transferred. In contrast, the platinum derivative (**2b**) showed a concentration-dependent equilibrium where the most abundant species was always the triangle $(2\text{bL})_3$, in agreement with our previous results with this phosphine. Thus, the triangular/square molar ratio decreased from about 10:1 (1 mM) to 2:1 (100 mM). The different results obtained on changing the metal from palladium to platinum confirm the great tendency of the palladium compounds to yield preferentially the thermodynamically favoured products (squares) as a result of the reversibility of the Pd(II)–pyridine bond.

The $^{31}\text{P}\{^1\text{H}\}$ -NMR spectrum of the solution obtained on mixing stoichiometric amounts of *cis*- $[\text{Pt}(\text{OTf})_2(\text{depe})]$ (**3b**) and **L** in CH_2Cl_2 (1 mM) showed one peak at $\delta(^{31}\text{P}) = 45.5$ ppm ($J(\text{PtP}) = 3130$ Hz). The resonance of this solution in the $^{195}\text{Pt}\{^1\text{H}\}$ -NMR spectrum appeared as a triplet centred at -4682 ppm. These peaks could be assigned to the triangle $(3\text{bL})_3$ on the basis of concentration dependence studies. Thus, the $^{31}\text{P}\{^1\text{H}\}$ -NMR spectrum of solutions of higher concen-

trations, showed, along with the peak at $\delta(^{31}\text{P}) = 45.5$ ppm, a new signal (square $(3\text{bL})_4$) at 45.1 ppm ($J(\text{PtP}) = 3130$ Hz). The triangle/square ratio in a 10 mM solution was about 10:1 and decreased to 2.5:1 in a 100 mM solution. ^1H -NMR spectroscopy featured the same behaviour. The $^{195}\text{Pt}\{^1\text{H}\}$ -NMR spectrum presented two triplets at -4682 and -4671 ppm that were assigned to the triangle and the square, respectively. Again the ^{31}P resonance for the triangle entity $(3\text{bL})_3$ is seen downfield compared to that of $(3\text{bL})_4$ while opposite trend is seen in ^{195}Pt -NMR and ^1H -NMR (α -protons of pyridine). The study carried out with the palladium complex **3a** and **L** gave only one peak at $\delta(^{31}\text{P}) = 78.5$ ppm in the ^{31}P -NMR spectrum, that was not concentration-dependent. In this case, the lack of equilibrium in solution required an assignment based on the FAB(+) mass spectrum, whose most intense peak ($m/z = 937.3$) corresponded to the square entity $(3\text{bL})_4$ (see Section 3).

Finally, in order to find out the influence of a rigid diphosphine ligand, such as the dppbz, we attempted to prepare the metal triflate complexes *cis*- $[\text{Pd}(\text{OTf})_2(\text{dppbz})]$ and $[\text{Pt}(\text{OTf})_2(\text{dppbz})]$. The bite angle of this diphosphine has not been reported, but probably will little differ from that of the dppe [11]. Despite the fact that we were able to prepare the palladium complex, the analogous platinum derivative could not be synthesised since we were unable to abstract efficiently the halides from $[\text{PtCl}_2(\text{dppbz})]$. The self-assembly of the palladium complex **4a** and **L** (Fig. 2) rendered a mixture of two species, according to the ^{31}P -NMR spectrum: $\delta(^{31}\text{P}) = 59.4$ ppm (triangle $(4\text{aL})_3$) and 58.7 ppm (square $(4\text{aL})_4$) in a dilute solution (1 mM) with a triangular/square ratio of 2.5:1, which varies to 1.2:1 for the 10 mM solution. However, the $^{31}\text{P}\{^1\text{H}\}$ -NMR spectrum of a 100 mM solution showed only a signal at 58.7 ppm, indicating that the equilibrium is totally shifted towards the thermodynamically more stable square entity.

The results reported here confirm the decisive influence of the linear bridging ligand in the assembly process. Although in our previous studies with **L** = 1,4-bis(4-pyridyl)tetrafluorobenzene the bite angle of the diphosphine ligand seemed to play an important role, the use of the longer, more basic and more flexible 1,4-bis(4-pyridyl)butadiyne has demonstrated the major influence of the activation energy for the breaking of the metal–pyridine bond and the dominance of entropic factors at low concentrations.

The reason why in some cases the less-favoured thermodynamical triangles resulted to be the predominant species at high concentrations could not be inferred from these experiments demonstrating once more that we are still far from being able to completely understand the factors that drive the self-assembly process to completion.

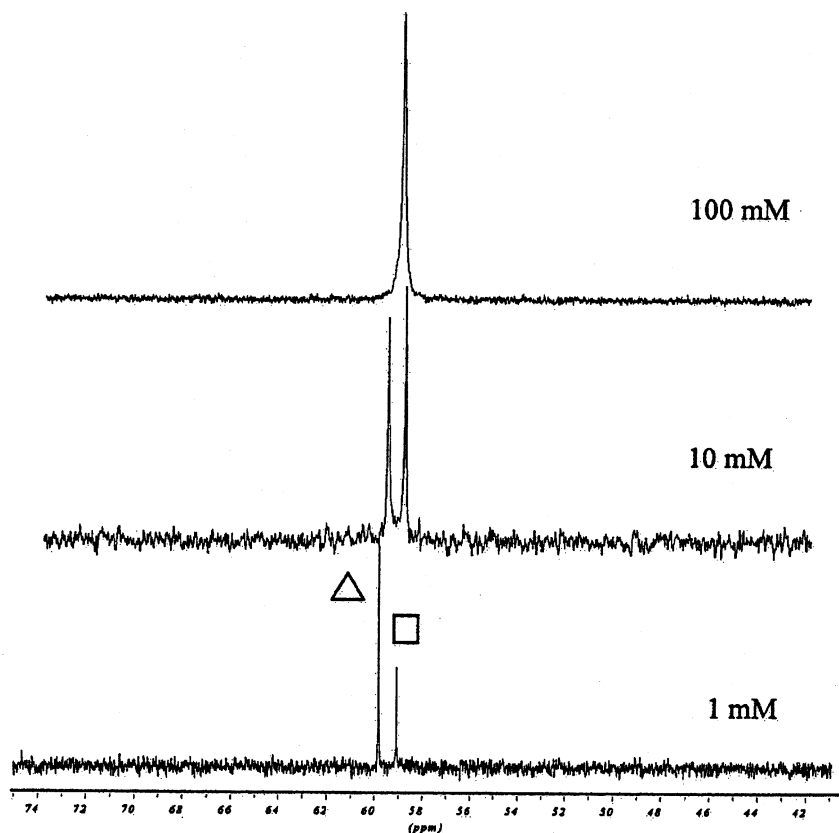


Fig. 2. $^{31}\text{P}\{^1\text{H}\}$ spectra of $(4\text{aL})_3/(4\text{aL})_4$ at different concentrations in CH_2Cl_2 solution.

2.2. Host–guest studies

Many macrocyclic complexes have been studied for their molecular recognition capabilities toward small aromatic molecules [1,2e,2f,2g,2h,9b,12,13], inorganic anions [2f,2g,2h,13,14] and porphyrin molecules [14e] based on the large cavity sizes and intermolecular forces or electrostatic interactions of these species. The macrocycles described here were supposed to be effective hosts for molecular recognition because of their overall positive charge and size. The investigation of the host–guest interactions of inorganic macrocycles can be achieved either by studying the changes in NMR chemical shifts and/or the changes in the excited-state emission intensity.

Preliminary experiments were carried out with solutions of the prepared macrocycles in CD_3NO_2 in an attempt to recognise anions such as PF_6^- or OTf^- . However, they did not show any significant binding interactions according to ^1H - and ^{31}P -NMR spectroscopy.

In order to study this kind of interactions by photochemistry, luminescence studies of compounds **1–4a**, **1–3b**, **L** and their corresponding metallamacrocycles were undertaken in dichloromethane solution at room temperature. Significantly, only **(1b+L)** and **(3b+L)** solutions exhibited luminescence emission while the

rest of species did not display detectable luminescence (Table 1). In fact, the reason for the non-emissive behaviour of the Pd(II) in front of Pt(II) compounds is unknown, although higher quantum yields have been reported for Pt(II) diphosphine-containing complexes by comparison with their Pd(II) analogue [15]. Otherwise, the lack of luminescence for the dppf-containing species could be ascribed to the quenching effect exerted by the $(\text{dppf})\text{M}(\text{II})$ moieties [2h,14a].

Time-correlated single photon counting measurements were carried out for 10^{-6} M solutions of **(1b+L)** and **(3b+L)**. The emission decays collected at 400 nm ($\lambda_{\text{exc}} = 337$ nm) are best fitted with only one exponential and this fact confirms that at this concentration only one emitting species is present in the solutions. Consequently, the lifetime measured should be attributed to the triangular species: $\tau(\mathbf{1bL})_3 = 310$ ps and $\tau(\mathbf{3bL})_3 = 200$ ps. The short decay times and the small Stokes shifts observed for these compounds (Fig. 3) suggest that the observed emission is a fluorescence phenomenon. This is in clear contrast with the results reported for the analogous $[\text{ReCl}(\text{CO})_3\text{L}]_4$ ($\tau = 39$ ns), **L** being the same ligand as the one used here, whose luminescence originates from the lowest $^3\text{MLCT}$ state and the Stokes shift is reported to be larger [9].

Luminescence titrations with either AgOTf or NBu_4PF_6 were found to affect the intensity emission

Table 1
Electronic absorption and emission data at 298 K in CH₂Cl₂ solution for compounds (**1bL**)₃ and (**3bL**)₃

Compound	Absorption spectra	Emission spectra			
	λ_{max} (nm) (ϵ , $\times 10^{-3} \text{ M}^{-1} \text{ cm}^{-1}$)	λ_{exc} (nm)	λ_{max} (nm)	ϕ ($\times 10^{-3}$)	τ (ps)
(1bL) ₃	305 (36.2), 326 (54.6), 350 (45.4)	350	398	9.1	200
(3bL) ₃	304 (36.3), 325 (66.0), 349 (53.2)	350	399, 424	15.0	310

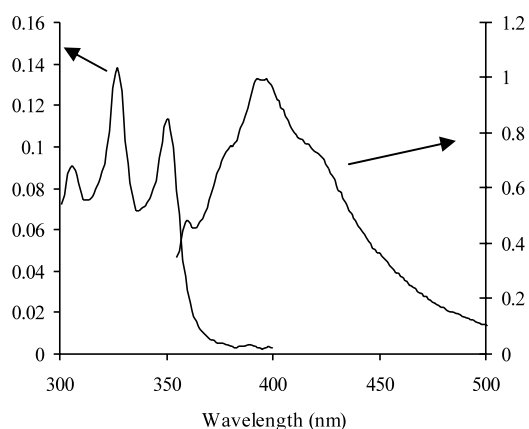


Fig. 3. Absorption (left) and emission (right) spectra of compound (**1bL**)₃.

of the receptors. That is, the addition of PF₆⁻ to a 2.5 × 10⁻⁶ M solution of the macrocycle (**3bL**)₃ in dichloromethane was found to cause an initial enhancement of the emission intensity of 35% followed by a decrease of the luminescence intensity that finally reaches the original value of the emission. In the case of (**1bL**)₃ a 10% quenching of the luminescence was observed. It should be noted that the emission position and band shape do not change with the anion binding.

However, two different responses were observed upon addition of OTf in the same conditions as those described above: i.e. while (**1bL**)₃ undergoes a 30% quenching of the luminescence emission (Fig. 4), (**3bL**)₃ displays a 55% increase of the emission intensity together with a slight red shift of the wavelength from 389 to 397 nm (Fig. 5).

Since the reports dealing with the recognition of these anions by macrocycles are to date very few in number [14a,14e,16], the physical basis of why PF₆⁻ and OTf⁻ induce different changes in the luminescence of the triangular compounds is not certain at this stage and deserves further investigation. As noted by other authors, presumably the anionic component of the added electrolyte interacts coulombically with the positive charge of the host cavity causing changes in the emission properties and undetectable variations in the NMR chemical shifts of the receptors.

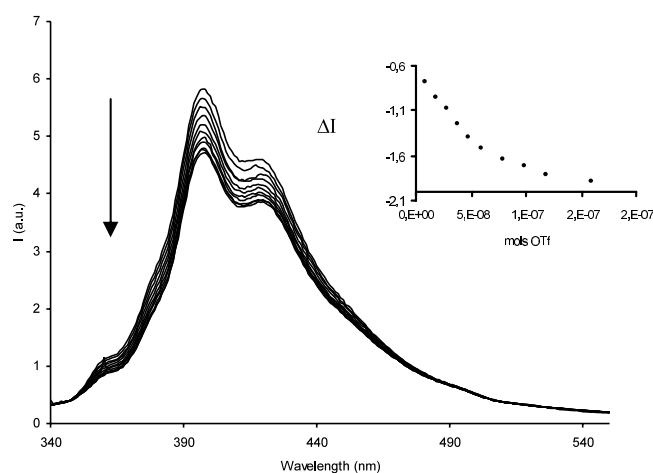


Fig. 4. Emission spectral variations upon titration of a CH₂Cl₂ solution of (**1bL**)₃ (2.5 × 10⁻⁶ M) with AgOTf.

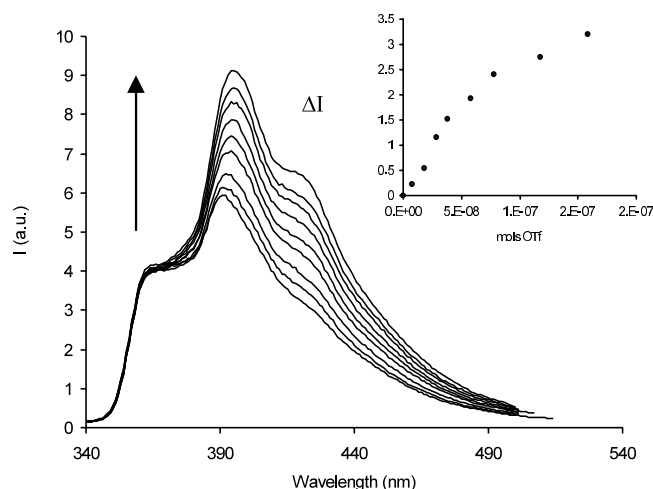


Fig. 5. Emission spectral variations upon titration of a CH₂Cl₂ solution of (**3bL**)₃ (2.5 × 10⁻⁶ M) with AgOTf.

3. Experimental

All manipulations were performed under prepurified N₂ using standard Schlenk techniques. All solvents were distilled from appropriate drying agents. Infrared spectra were recorded on an FTIR 520 Nicolet spectrophotometer. ³¹P{¹H}-NMR (δ (85% H₃PO₄) = 0 ppm), ¹⁹⁵Pt{¹H}-NMR (δ (K₂[PtCl₆]) = 0 ppm) and ¹H-NMR (δ (TMS) = 0 ppm) spectra were obtained on a Bruker

DXR 250 and Varian 200 spectrometers. Elemental analyses of C, H, N and S were carried out at the Serveis Científic-Tècnics in Barcelona. FAB(+) and electro-spray mass spectra were recorded on a Fisons VG Quattro spectrometer.

Absorption spectra were recorded on a Shimadzu UV-2510 PC, UV-vis recording spectrophotometer, and fluorescence emission on an SPEX F111 Fluorolog spectrofluorimeter and on an SLM AMINCO Bowman Series 2 luminescence spectrometer. Total luminescence quantum yields were measured relatively to anthracene, $\phi = 0.36$. Luminescence decays were obtained with an Applied Photophysics laser flash photolysis equipment pumped by an Nd:YAG laser (Spectra Physics) with excitation at 355 nm.

Electrochemical measurements for the dppf complexes were recorded on a Princeton Applied Research Model 263A potentiostat (EG&G instruments). The electrochemical cell consisted of a platinum disk working electrode (TACUSSEL-EDI rotatory electrode (3.14 mm²)), a platinum wire auxiliary electrode and a Ag/AgNO₃ (0.1 M, in acetonitrile solution) reference electrode separated from the solution by a medium porosity fritted disk. Cyclic voltammograms were obtained from 5×10^{-4} M solutions of the samples under nitrogen at 25 °C using dry CH₂Cl₂ as solvent and tetrabutylammonium hexafluorophosphate (0.1 M) as supporting electrolyte. For electrolysis experiments a Pt gauze was used. Ferrocene (Fc) was used as an internal reference with the redox couple Fc/Fc⁺ occurring at 0.15 V.

The compounds 1,4-bis(4-pyridyl)butadiyne [17], [Pt(dppp)(H₂O)₂](OTf)₂ [12c], [Pd(dppp)(H₂O)₂](OTf)₂ [12c], [Pt(dppf)(H₂O)₂](OTf)₂ [7] and [Pd(dppf)(H₂O)₂](OTf)₂ [7] were prepared as described previously. [Pt(depe)(OTf)₂], [Pd(depe)(OTf)₂] and [Pd(dppbz)(OTf)₂] were synthesised by similar methods.

Inorganic anion binding studies for the (1bL)₃ and (3bL)₃ metallacycles were conducted in dichloromethane solutions using luminescence detection. A 2.5×10^{-6} M solution of the complex in dichloromethane was prepared and a 3 cm³ portion was transferred to a 1 cm fluorescent cell. Small aliquots from a 10⁻³ M solution of the anion in dichloromethane were added to the cell. The changes in luminescence intensity were monitored as a function of the guest molar number.

3.1. Synthesis of metallacycles (1bL)₄/(1bL)₃

Solid 1,4-bis(4-pyridyl)butadiyne (15 mg, 0.073 mmol) was added to a CH₂Cl₂ (7 cm³) solution of [Pt(dppp)(H₂O)₂](OTf)₂ (69 mg, 0.073 mmol) at room temperature. After 2 h of stirring, the reaction mixture was concentrated to 2 cm³ under vacuum and diethyl-ether was added (15 cm³). After filtration a white solid was obtained (81 mg, 96%).

(1bL)₄: ¹H-NMR (nitromethane-*d*₃): δ 8.83 (m, 16H, H _{α} -pyr), 7.80–7.38 (m, 80H, Ph), 7.25 (m, 16H, H _{β} -pyr), 3.36 (s, br, 16H, P-CH₂-), 2.40 (m, br, 8H, P-CH₂-CH₂-). ³¹P{¹H}-NMR (nitromethane-*d*₃): δ -14.9 (s, $J(\text{PtP}) = 3022$ Hz). ¹⁹⁵Pt{¹H}-NMR (nitromethane-*d*₃): δ -4421 (t, $J(\text{PtP}) = 3022$ Hz).

(1bL)₃: ¹H-NMR (nitromethane-*d*₃): δ 8.62 (d, $J = 2.7$ Hz, 12H, H _{α} -pyr), 7.80–7.38 (m, 60H, Ph), 7.26 (m, 12H, H _{β} -pyr), 3.36 (s, br, 12H, P-CH₂-), 2.40 (m, br, 6H, P-CH₂-CH₂-). ³¹P{¹H}-NMR (nitromethane-*d*₃): δ -14.5 (s, $J(\text{PtP}) = 3021$ Hz). ¹⁹⁵Pt{¹H}-NMR (nitromethane-*d*₃): δ -4436 (t, $J(\text{PtP}) = 3021$ Hz).

(1bL)₄/(1bL)₃: Anal. Found: C, 46.40; H, 3.41; N, 2.70; S, 6.00. (C₄₃H₃₄F₆N₂O₆P₂PtS₂)_{*n*} ($n = 1109.09$) requires C, 46.52; H, 3.10; N, 2.52; S, 5.77%. IR (KBr, cm⁻¹): $\nu(\text{C}\equiv\text{C})$, 2164 m, 2145 m; OTf⁻, 1260 vs, 1156 s, 1101 s, 1029 vs. ES mass spectrum (CH₃NO₂, *m/z*): 406.1 [(dppp)PtL]²⁺, 960.8 [(1bL)₄-4OTf⁻]⁴⁺ or [(1bL)₃-3OTf⁻]³⁺.

3.2. Syntheses of metallacycles (1aL)₄/(1aL)₃, (2bL)₄/(2bL)₃, (2aL)₄, (3bL)₄/(3bL)₃, (3aL)₄ and (4aL)₄/(4aL)₃

Details of synthesis of (1bL)₄/(1bL)₃ also apply to these compounds.

(1aL)₄: ¹H-NMR (nitromethane-*d*₃): δ 8.73 (d, $J = 4.4$ Hz, 16H, H _{α} -pyr), 7.84–7.32 (m, 80H, Ph), 7.22 (m, 16H, H _{β} -pyr), 3.27 (s, br, 16H, P-CH₂-), 2.30 (m, br, 8H, P-CH₂-CH₂-). ³¹P{¹H}-NMR (nitromethane-*d*₃): δ 7.5 (s).

(1aL)₃: ¹H-NMR (nitromethane-*d*₃): δ 8.63 (d, $J = 5.8$ Hz, 12H, H _{α} -pyr), 7.84–7.32 (m, 60H, Ph), 7.22 (m, 12H, H _{β} -pyr), 3.27 (m, 12H, P-CH₂-), 2.30 (m, br, 6H, P-CH₂-CH₂-). ³¹P{¹H}-NMR (nitromethane-*d*₃): δ 8.1 (s).

(1aL)₄/(1aL)₃: pale green solid. Yield: 95%. Anal. Found: C, 50.62; H, 3.37; N, 2.87; S, 6.73. (C₄₃H₃₄F₆N₂O₆P₂PdS₂)_{*n*} ($n = 1020.40$) requires C, 50.57; H, 3.33; N, 2.74; S, 6.27%. IR (KBr, cm⁻¹): $\nu(\text{C}\equiv\text{C})$, 2220 m, 2150 m, 1257 vs; OTf⁻, 1159 s, 1103 s, 1029 vs. ES mass spectrum (CH₃NO₂, *m/z*): 360.7 [Pd(dppp)L]²⁺, 666.7 [(1aL)₄-5OTf⁻]⁵⁺.

(2aL)₄: violet solid. Yield: 97%. ¹H-NMR (CDCl₃): δ 8.80 (m, 16H, H _{α} -pyr), 7.86–7.56 (m, 80H, Ph), 6.97 (d, $J = 5.87$ Hz, 16H, H _{β} -pyr), 4.82 (s, 16H, H _{α} -Fc), 4.59 (s, 16H, H _{β} -Fc). ³¹P{¹H}-NMR (CH₂Cl₂, inset acetone-*d*₆ with 1% POME₃): δ 32.8 (s). ES mass spectrum (CH₂Cl₂, *m/z*): 432.0 [Pd(dppf)L]²⁺, 534.2 [(2aL)₄+H⁺]-6OTf⁻]⁵⁺, 782.0 [(2aL)₄-5OTf⁻]⁵⁺, 809.2 [(2aL)₄+H⁺]-4OTf⁻]⁵⁺, 1400.1 [(2aL)₄-3OTf⁻]³⁺. Cyclic voltammetry (CH₂Cl₂, [Pd] = 5×10^{-4} M): $E_{1/2} = 0.81$ V. Anal. Found: C, 51.73; H, 3.32; N, 2.28; S, 5.53. (C₅₀H₃₆F₆FeN₂O₆P₂PdS₂)_{*n*} ($n = 1162.79$) requires C, 51.60; H, 3.27; N, 2.24; S, 5.50%. IR (KBr, cm⁻¹): $\nu(\text{C}\equiv\text{C})$, 2221 m, 2165 m, 2144 m; OTf⁻, 1257 vs, 1160 s, 1103 s, 1030 vs.

(2bL)₄: ¹H-NMR (nitromethane-*d*₃): δ 8.46 (m, 16H, H_{α-pyr}), 7.93–7.56 (m, 80H, Ph), 7.33 (d, *J* = 16.80 Hz, 16H, H_{β-pyr}), 4.77 (s, br, 16H, H_{α-Fc}), 4.60 (s, 16H, H_{β-Fc}). ³¹P{¹H}-NMR (CH₂Cl₂, inset acetone-*d*₆ with 1% POME₃): δ 2.7 (s, *J*(PtP) ≅ 3460 Hz: satellites are obscured and overlap with the signals of the triangle). ¹⁹⁵Pt{¹H}-NMR (nitromethane-*d*₃): δ -4252 (t, *J*(PtP) = 3460 Hz).

(2bL)₃: ¹H-NMR (nitromethane-*d*₃): δ 8.33 (d, *J* = 4.3 Hz, 12H, H_{α-pyr}), 7.93–7.56 (m, 60H, Ph), 7.15 (d, 12H, H_{β-pyr}), 4.77 (s, br, 16H, H_{α-Fc}), 4.69 (s, 16H, H_{β-Fc}). ³¹P{¹H}-NMR (nitromethane-*d*₃): δ 2.8 (s, *J*(PtP) = 3461 Hz). ¹⁹⁵Pt{¹H}-NMR (nitromethane-*d*₃): δ -4261 (t, *J*(PtP) = 3461 Hz). Cyclic voltammetry (CH₂Cl₂, [Pt] = 5 × 10⁻⁴ M): *E*_{1/2} = 0.88 V.

(2bL)₄/**(2bL)₃**: orange solid. Yield: 94%. Anal. Found: C, 46.08; H, 3.07; N, 2.28; S, 5.14. (C₅₀H₃₆F₆FeN₂O₆P₂PtS₂)_{*n*} (*n* = 1251.48) requires C, 46.03; H, 3.04; N, 2.24; S, 5.11%. IR (KBr, cm⁻¹): ν(C≡C), 2228 m, 2171 m, 2151 m; OTf⁻, 1257 vs, 1161 s, 1104 s, 1030 vs. ES mass spectrum (CH₂Cl₂, *m/z*): 827.7 [(**(2bL)**₃ + H⁺) - 3OTf⁻]⁴⁺, 882.0 [(**(2bL)**₄ + H⁺) - 4OTf⁻]⁵⁺, 1103.2 [(**(2bL)**₃ - 3OTf⁻]³⁺ or [(**(2bL)**₄ - 4OTf⁻]⁴⁺, 1140.6 [(**(2bL)**₄ + H⁺) - 3OTf⁻]⁴⁺.

(3aL)₄: white solid. Yield: 75%. ¹H-NMR (nitromethane-*d*₃): δ 8.85 (br, 16H, H_{α-pyr}), 7.68 (br, 16H, H_{β-pyr}), 2.47 (m, 16H, P-(CH₂)₂), 2.16 (m, 32H, P-CH₂-CH₃), 1.26 (dt, *J*(PH) = 18.6 Hz, *J*(HH) = 7.5 Hz, 48H, P-CH₂-CH₃). ³¹P{¹H}-NMR (nitromethane-*d*₃): δ 78.5 (s). FAB mass spectrum (CH₃NO₂, *m/z*): 461.1 [(depe)Pd(OTf)]⁺, 666.2 [(**(3aL)**₄ - 4OTf⁻]⁴⁺, 937.3 [(**(3aL)**₄ - 3OTf⁻]³⁺. Anal. Found: C, 38.52; H, 3.87; N, 3.51; S, 7.91. (C₂₆H₃₂F₆N₂O₆P₂PdS₂)_{*n*} (*n* = 814.65) requires C, 38.30; H, 3.92; N, 3.44; S, 7.86%. IR (KBr, cm⁻¹): ν(C≡C), 2166 m, 2143 m; OTf⁻, 1260 vs, 1178 s, 1102 m, 1032 vs.

(3bL)₄: ¹H-NMR (nitromethane-*d*₃): δ 8.91 (m, 16H, H_{α-pyr}), 7.80 (d, *J* = 5.9 Hz, 16H, H_{β-pyr}), 2.26 (m, 16H, P-(CH₂)₂), 2.10 (m, 32H, P-CH₂-CH₃), 1.25 (dt, *J*(PH) = 18.7 Hz, *J*(HH) = 8.1 Hz, 48H, P-CH₂-CH₃). ³¹P{¹H}-NMR (nitromethane-*d*₃): δ 37.6 (s, *J*(PtP) = 3130 Hz). ¹⁹⁵Pt{¹H}-NMR (nitromethane-*d*₃): δ -4671 (t, *J*(PtP) = 3130 Hz).

(3bL)₃: ¹H-NMR (nitromethane-*d*₃): δ 8.87 (m, 12H, H_{α-pyr}), 7.75 (d, *J* = 5.9 Hz, 12H, H_{β-pyr}), 2.26 (m, 12H, P-(CH₂)₂), 2.10 (m, 24H, P-CH₂-CH₃), 1.25 (dt, *J*(PH) = 18.7 Hz, *J*(HH) = 8.1 Hz, 36 H, P-CH₂-CH₃). ³¹P{¹H}-NMR (nitromethane-*d*₃): δ 37.9 (s, *J*(PtP) = 3130 Hz). ¹⁹⁵Pt{¹H}-NMR (nitromethane-*d*₃): δ -4682 (t, *J*(PtP) = 3130 Hz).

(3bL)₄/**(3bL)₃**: white solid. Yield: 75%. Anal. Found: C, 34.70; H, 3.57; N, 3.12; S, 7.21. (C₂₆H₃₂F₆N₂O₆P₂PtS₂)_{*n*} (*n* = 903.34) requires C, 34.54; H, 3.54; N, 3.10; S, 7.08%. IR (KBr, cm⁻¹): ν(C≡C), 2165 m, 2144 m; OTf⁻, 1261 vs, 1180 s, 1102 m, 1035 vs.

ES mass spectrum (CH₃NO₂, *m/z*): 303.7 [Pt(depe)L]²⁺, 318.8 [(**(3bL)**₄ + H⁺) - 6OTf⁻]⁷⁺, 756.6 [(**(3bL)**₃ - 3OTf⁻]³⁺ or [(**(3bL)**₄ - 4OTf⁻]⁴⁺.

(4aL)₄: ¹H-NMR (nitromethane-*d*₃): δ 8.60 (m, 16H, H_{α-pyr}), 8.15–7.98 (m, 16H, P-C₆H₄-P), 7.71–7.38 (m, 80H, Ph), 7.16 (m, 16H, H_{β-pyr}). ³¹P{¹H}-NMR (CH₂Cl₂, inset acetone-*d*₆ with 1% POME₃): δ 58.7 (s).

(4aL)₃: ¹H-NMR (nitromethane-*d*₃): δ 8.48 (m, 12H, H_{α-pyr}), 8.15–7.98 (m, 12H, P-C₆H₄-P), 7.71–7.38 (m, 60H, Ph), 7.11 (m, 12H, H_{β-pyr}). ³¹P{¹H}-NMR (CH₂Cl₂, inset acetone-*d*₆ with 1% POME₃): δ 59.4 (s).

(4aL)₄/**(4aL)₃**: white solid. Yield: 95%. Anal. Found: C, 52.51; H, 3.07; N, 2.69; S, 6.13. n(C₄₆H₃₂F₆N₂O₆P₂PdS₂) (*n* = 1054.87) requires C, 52.34; H, 3.03; N, 2.65; S, 6.07%. IR (KBr, cm⁻¹): ν(C≡C), 2225 m, 2170 m, 2148 m; OTf⁻, 1257 vs, 1155 vs, 1101 s, 1030 vs. FAB mass spectrum (CH₃NO₂, *m/z*): 552.1 [(**(4aL)**₄ - 6OTf⁻]⁶⁺, 905.1 [(**(4aL)**₃ - 3OTf⁻]³⁺ or [(**(4aL)**₄ - 4OTf⁻]⁴⁺.

Acknowledgements

This work was supported by DGICYT (Project BQU2000-0644) and CIRIT (Project 2001 SGR 00054). L.R. is indebted to the Universitat de Barcelona for a scholarship. We thank Dr. João C. Lima for decay time measurements.

References

- [1] M. Fujita, J. Yazaki, K. Ogura, *J. Am. Chem. Soc.* 112 (1990) 5645.
- [2] See for example: (a) B. Olenyuk, A. Fechtenkötter, P.J. Stang, *J. Chem. Soc. Dalton Trans.* (1998) 1707; (b) M. Fujita, K. Ogura, *Bull. Chem. Soc. Jpn.* 69 (1996) 1471; (c) F.A. Cotton, C. Lin, C.A. Murillo, *Acc. Chem. Res.* 34 (2001) 759; (d) G.F. Swiegers, T.J. Malefetse, *Chem. Rev.* 100 (2000) 3483; (e) M. Fujita, *Chem. Soc. Rev.* 27 (1998) 417; (f) S. Leininger, B. Olenyuk, P.J. Stang, *Chem. Rev.* 100 (2000) 853; (g) B.J. Holliday, C.A. Mirkin, *Angew. Chem. Int. Ed. Engl.* 40 (2001) 2023; (h) S.-S. Sun, A.J. Lees, *Coord. Chem. Rev.* 230 (2002) 171
- [3] (a) M. Fujita, O. Sasaki, T. Mitsunashi, T. Fujita, J. Yazaki, K. Yamaguchi, K. Ogura, *Chem. Commun.* (1996) 1535; (b) S.B. Lee, S. Hwang, D.S. Chung, H. Yun, J.-I. Hong, *Tetrahedron Lett.* 39 (1998) 873; (c) M. Schweiger, S. Russell, A.M. Arif, P.J. Stang, *Inorg. Chem.* 41 (2002) 2556; (d) A. Sautter, D.G. Schmid, G. Jung, F. Würthner, *J. Am. Chem. Soc.* 123 (2001) 5424; (e) C.A. Schalley, T. Müller, P. Linnartz, M. Witt, M. Schäfer, A. Lützen, *Chem. Eur. J.* 8 (2002) 3538; (f) K.-M. Park, S.-Y. Kim, J. Heo, D. Whang, S. Sakamoto, K. Yamaguchi, K. Kim, *J. Am. Chem. Soc.* 124 (2002) 2140; (g) F.M. Romero, R. Ziessel, A. Dupont-Gervais, A. van Dorsselaer, *Chem. Commun.* (1996) 551.

- [4] X. Chi, A.J. Guerin, R.A. Haycock, C.A. Hunter, L.D. Sarson, *Chem. Commun.* (1995) 2567.
- [5] M. Schweiger, S.R. Seidel, A.M. Arif, P.J. Stang, *Angew. Chem. Int. Ed. Engl.* 40 (2001) 3467.
- [6] M. Ferrer, M. Mounir, O. Rossell, E. Ruiz, M.A. Maestro, *Inorg. Chem.*, in press.
- [7] P.J. Stang, B. Olenyuk, J. Fan, A.M. Arif, *Organometallics* 15 (1996) 904.
- [8] F. Würthner, A. Sautter, *Chem. Commun.* (2000) 445.
- [9] (a) S.-S. Sun, A.J. Lees, *Inorg. Chem.* 38 (1999) 4181;
(b) S.-S. Sun, A.J. Lees, *J. Am. Chem. Soc.* 122 (2000) 8956.
- [10] The molarity is based on the mols of the metal (Pd or Pt).
- [11] P. Dierkes, P.W.N.M. Van Leeuwen, *J. Chem. Soc. Dalton Trans.* (1999) 1519.
- [12] See for example: (a) M. Fujita, J. Yakazi, K. Ogura, *Tetrahedron Lett.* 32 (1991) 5589;
(b) M. Fujita, S. Nagao, M. Iida, K. Ogura, *J. Am. Chem. Soc.* 115 (1993) 1574;
(c) P.J. Stang, K. Chen, A.M. Arif, *J. Am. Chem. Soc.* 117 (1995) 6273;
(d) P. de Wolf, S.L. Heath, J.A. Thomas, *Chem. Commun.* (2002) 2541
- [13] A.P. De Silva, H.Q. Gunaratne, N.T. Gunnlaugsson, A.J.M. Huxley, C.P. McCoy, J.T. Rademacher, T.E. Rice, *Chem. Rev.* 97 (1997) 1515.
- [14] See for example: (a) S.-S. Sun, J.A. Anspach, A.J. Lees, P.Y. Zavalij, *Organometallics* 21 (2002) 685;
(b) P.D. Beer, V. Timoshenko, M. Maestri, P. Passaniti, V. Balzani, *Chem. Commun.* (1999) 1755.;
(c) P.D. Beer, F. Szemes, V. Balzani, C.M. Sala, M.G.B. Drew, S.W. Dent, M. Maestri, *J. Am. Chem. Soc.* 119 (1997) 11864;
(d) R.V. Slone, K.D. Benkstein, S. Bélanger, J.T. Hupp, I.A. Guzei, A.L. Rheingold, *Coord. Chem. Rev.* 171 (1998) 221;
(e) P.D. Beer, *Acc. Chem. Res.* 31 (1998) 71;
(f) R.V. Slone, D.I. Yoon, R.M. Calhoun, J.T. Hupp, *J. Am. Chem. Soc.* 117 (1995) 11813
- [15] D. Xu, H.J. Murfee, W.E. Van der Veer, B. Hong, *J. Organomet. Chem.* 596 (2000) 53.
- [16] (a) Z. Qin, M.C. Jennings, R.J. Puddephat, *Inorg. Chem.* 41 (2002) 3967;
(b) R.-D. Schnebeck, E. Freisinger, B. Lippert, *Angew. Chem. Int. Ed. Engl.* 38 (1999) 165.
- [17] L.D. Ciana, A. Haim, *J. Heterocycl. Chem.* 21 (1984) 607.